Thermal-hydraulic digester model using a higher order numerical method

Sharad Bhartiya, Pascal Dufour, Francis J. Doyle Iii

1
University of Delaware,
Department of Chemical Engineering,
Newark, DE 19716, USA
http://www.udel.edu

THERMAL-HYDRAULIC DIGESTER MODEL USING A HIGHER ORDER NUMERICAL METHOD

Sharad Bhartiya, Pascal Dufour and Francis J. Doyle III[1]

Department of Chemical Engineering
University of Delaware
Newark DE 19711

Key words: continuous pulp digester, first principles modeling, distributed parameter system, numerical method

Prepared for Presentation at the 2001 Annual Meeting, Reno, Nevada, Nov. 5 – Nov. 9
Session: Simulation and Process Control in Forest Products Industry
Unpublished

[1] Corresponding author: Fax (302) 831 1048; Phone (302) 831 0760; email fdoyle@udel.edu

Abstract

This paper presents a detailed fundamental model of a continuous pulp digester developed for simulation and control. Most modeling efforts in the past have either emphasized on reaction kinetics and energy transfer assuming a prescribed flow behavior, or modeled digester hydraulics with simplified reaction kinetics. In this work, we augment the well-known Purdue model by incorporating axial momentum transport, an immediate consequence of which is ability to simulate chip level and its impact on the Kappa number profile. Model performance is illustrated using simulation. The current work also explores and illustrates the use of higher order finite difference methods to reduce numerical dissipation and dispersion.

Key words: continuous pulp digester, first principles modeling, distributed parameter system, numerical method

1. INTRODUCTION

Pulping mills convert wood chips to pulp suitable for paper production by displacing lignin from cellulose fibers. The conversion is achieved through a combination of strategies involving thermal, chemical and mechanical degradation of the wood chips. Continuous Kraft processes use large, vertical, tubular reactors called digesters where the chips react with an aqueous solution of sodium hydroxide and sodium sulfide, known as white liquor, at elevated temperature. Most continuous digesters consist of three basic zones: an impregnation zone, a cooking zone and a wash zone. A schematic of a single vessel digester is shown in Fig. 1. White liquor and pre-steamed chips are introduced at the top of the digester into the impregnation zone where the liquor penetrates the wet chips. However, the majority of the delignification reaction occurs only after the two streams flow downward into the subsequent cooking zone where the mixture is heated to reaction temperatures achieved by liquor circulation through external heaters. The spent liquor is withdrawn from the digester at extraction screens located at the end of the cook zone while the cooked chips continue the downward journey to the wash zone. Here, the chips are washed by the countercurrent flow of cold, dilute liquor. This effectively quenches the delignification reaction. The quality of the resulting pulp is described by Kappa #, which is a measure of the residual lignin content. A typical control objective of digester operation is to minimize variation in the Kappa # from a prescribed value. Continuous digesters present challenging problems in modeling and control. From a modeling perspective, the inter-play between heat, mass and momentum transport during the thermal-hydraulic degradation of the wood chips makes the system coupled. For example, softening of the chips, as cooking proceeds, causes them to compact more densely which in turn affects the chip velocity profiles.

The capital-intensive nature of the pulp & paper industry mandates development of operating strategies that use enhanced control, soft-sensing and fault diagnosis methodologies, which are usually predicated on availability of a process model. A significant effort has been directed to development of first-principles models that describe the thermal-hydraulic degradation of wood chips in the continuous pulp digester. Most fundamental digester models in literature can be classified into two broad categories depending on the attributes they emphasize, 1) pulping chemistry; and 2) hydraulic description of the chip and liquor streams. Smith and Williams (1974) developed kinetic models based on pulping chemistry data. They then approximated the digester by a series of continuous stirred tank reactors (CSTRs) to obtain dynamic mass balances for the main components participating in pulping reactions. Each CSTR was assumed to contain three phases: 1) a solid phase consisting of the wood substance; 2) an entrapped liquor phase comprising of liquor in the pores of the wood chips; and 3) a bulk free liquor phase surrounding the wood chips. The resulting digester model is referred to as the Purdue model. The major contribution of the Purdue model was development of a framework upon which subsequent models could be based. Christensen *et al*. (1982) modified the Purdue model by incorporating improved kinetic parameters valid over a larger range of wood species. The wood substance was classified

as high and low reactive lignin, cellulose, galactoglucomannan and araboxylan. The improved model predicted free liquor concentration profiles and blow-line Kappa # for an industrial digester. An implementation of a commercialized model for model predictive control is reported by Christensen *et al.* (1994). Gustafson *et al*. (1983) developed alternate kinetic expressions to describe the delignification reaction. They use fewer number of wood and liquor components, and make use of functional relationships between rate of consumption of carbohydrates and lignin.

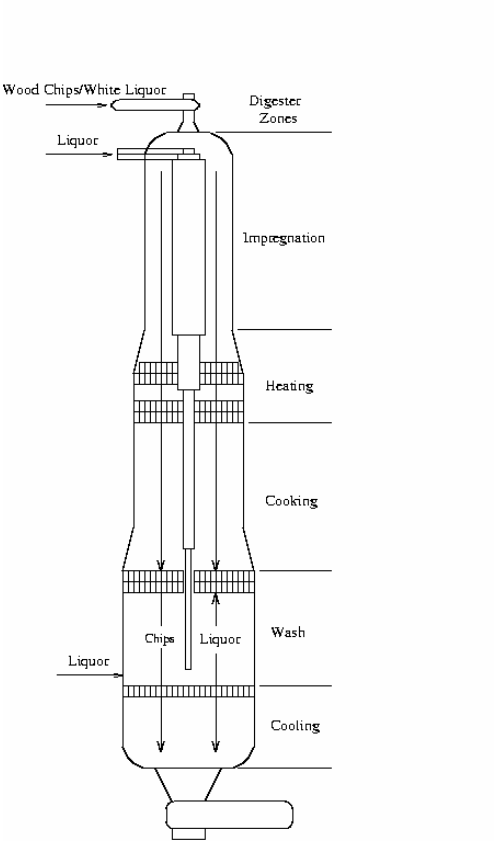

Fig 1. Schematic of a single vessel continuous digester.

Kayihan *et al.* (1996) presented a benchmark model for a two-vessel Kamyr digester with separate impregnation and reaction vessels. The model assumes two phases: nonporous solid and free liquor, which exist in thermal equilibrium. The kinetic model of Christensen *et al.* (1982) is adopted to describe dynamic mass balances. The resulting set of PDEs is discretized spatially and the model is solved as a system of ODEs. Extensions of the Purdue model have been presented by Wisnewski *et al.* (1997). They redefined mass concentrations and volume fractions that allowed relaxation of certain assumptions in the previous Purdue model leading to higher model fidelity.

In all of the preceding work, a steady, unchanging compaction profile is assumed. Further, these models fail to provide a dynamic description of chip level, an important control variable. This is a necessary consequence of absence of momentum transport modeling. On the other hand, hydraulic description based models assume simpler chemistry, constraining the validity to narrower ranges of Kappa #. Härkönen (1987) presented a detailed description of chip and liquor flow dynamics, and compaction, in addition to mass and energy transport. Constitutive equations that described flow resistance were developed experimentally. The resulting model was a system of two-dimensional PDEs that were solved at steady state. Simplifying assumptions are made with regards to the reaction kinetics and delignification in wood chips is ignored. Nevertheless, Härkönen's work laid the foundation for integrating digester hydraulics with existing models based on mass and energy transport. Michelsen (1995) proposed an integration of the works by Christensen *et al.* (1982) and Härkönen (1987) to develop a detailed digester model from mass, energy and axial momentum transport balances. The model assumes solid, entrapped liquor and free liquor phases in the digester and is described by a complex set of algebraic equations and PDEs. It is solved numerically using a staggered grid finite difference approach. While, chip and liquor flow dynamics are described in detail, simplifications are made in reaction kinetics, which constrain the validity of the model for Kappa # within the range of 50 and 150. A key result of Michelsen's model was ability to study the effect of flow behavior and compaction on Kappa #. Further, the study suggested residence time control could yield improved Kappa # control.

The model developed in this article is a direct integration of the works of Wisnewski *et al.* (1997) and Michelsen (1995) that overcomes some of the deficiencies described above. Thus, the detailed kinetics and mass/energy transport of the extended Purdue model are augmented with Michelsen's momentum transport description, yielding a thermal-hydraulic model of the continuous digester. The article is arranged as follows: section 2 outlines the derivation of the thermal-hydraulic model, section 3 discusses the first and fourth order finite difference techniques used for simulation, results and discussion are presented in section 4, followed by conclusions in section 5.

2. MODEL DERIVATION

The proposed model is based on a distributed parameter approach, where the axial distribution of transport properties occurs due to convection of the chips and liquor streams. Thermal and chemical gradients in radial direction are neglected. The temporal variations within each infinitesimal control volume are described by conservation statements, resulting in a set of coupled nonlinear PDEs. External flows from heaters and extraction screens are modeled as flows entering and/or leaving the control volume. The remainder of the section outlines the transport equations and constitutive rules used.

2.1 Physical Description

As in the Purdue model, each control volume is assumed to contain three phases: solid phase, entrapped liquor phase, and free liquor phase. The entrapped liquor phase resides within the pores of the wood chips where it reacts with the solid substance. However, dynamic and thermal equilibria are assumed between these two phases. In this work, the combined solid and entrapped liquor phases will be referred to as the chip phase. A schematic of an infinitesimal slice of the digester with volume ΔV is show in Fig. 2.

The results presented in Section 4 assume control volumes (CVs) with fixed cross-sectional areas, *A*. Inventory of each phase at a fixed vertical location in the digester is measured using the following volume fraction definitions,

$$\eta = \frac{\text{volume of free liquor phase in } \Delta V}{\text{volume of } \Delta V}\left[\frac{\Delta V_f(z)}{\Delta V(z)}\right]$$

The remainder of the control volume is assumed to be occupied by the chip phase. Thus,

$$(1-\eta) = \frac{\text{volume of chip phase in } \Delta V}{\text{volume of } \Delta V}\left[\frac{\Delta V_c(z)}{\Delta V(z)}\right]$$

The chip phase volume consists of the solid wood substance and entrapped liquor. The fraction of the chip phase occupied by entrapped liquor is then defined as the porosity,

$$\varepsilon = \frac{\text{volume of entrapped liquor phase in } \Delta V}{\text{volume of chip phase in } \Delta V}\left[\frac{\Delta V_e(z)}{\Delta V_c(z)}\right]$$

Equivalently,

$$(1-\varepsilon) = \frac{\text{volume of solid phase in } \Delta V}{\text{volume of chip phase in } \Delta V}\left[\frac{\Delta V_s(z)}{\Delta V_c(z)}\right]$$

As shown in Fig. 2, the chip phase enters the digester slice with volumetric flowrate $\dot{V}_c(z)$, and exits at a rate of $\dot{V}_c(z+\Delta z)$. Free liquor flows cocurrently, with the chip phase, in the cooking zone and countercurrently in the wash zone. Volumetric flow of free liquor is defined by $\dot{V}_f$. Chip and free liquor phase velocities are defined as,

$$\dot{V}_c = A(1-\eta)v_c$$
$$\dot{V}_f = A\eta v_f$$

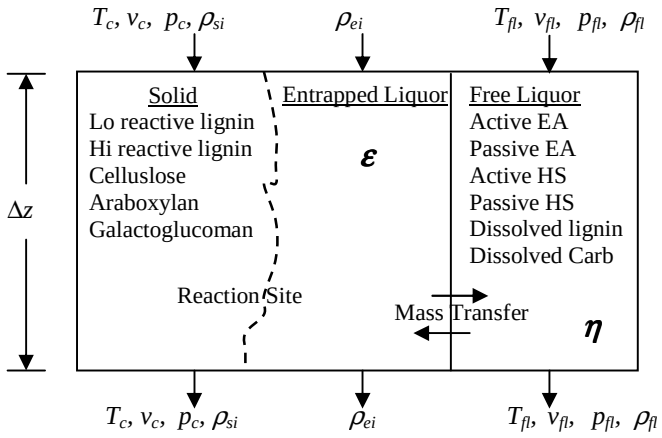

Fig. 2. A cross-sectional slice of digester consists of solid, entrapped liquor and free liquor phases.

respectively. Properties of external streams (for example, heater circulation streams) are referenced by the subscript *ext*. The free liquor pressure distribution, $P_f(z)$, is mainly dictated by the hydrostatic head in the digester. Depending on the degree of cooking, the chip phase at a given location, *z*, has a certain Kappa # associated with it. Härkönen (1987) performed experimental studies to evaluate the effect of cooking on the compactability of chips and then defined a chip pressure, p_c, which is the force that acts through the inter-chip contact points over a reference area. As noted by Michelsen (1995), the chips become softer during cooking enabling them to pack more tightly. The softening of chips is reflected by reduced chip pressure. Härkönen's work (1987) also suggests that while the chips become softer during cooking, they change shape but no appreciable change in volume occurs.

2.2 Solid Phase Mass Continuity

As in Purdue model (Christensen *et al.*, 1982), the solid phase is assumed to consist of five components: high-reactive lignin (s_1); low-reactive lignin (s_2); cellulose (s_3); araboxylan (s_4); and galactoglucomannan (s_5). Performing a component balance for the solid phase at location *z* yields the following,

$$\frac{\partial \rho_{si}}{\partial t} = -v_c \frac{\partial \rho_{si}}{\partial z} + \hat{R}_{si} \qquad (1)$$

where ρ_{si} denotes concentration of solid component *i* and is defined as the mass of component *i* in the solid phase per volume of chip phase. $\hat{R}_{si}$ represents the rate of consumption of mass of solid *i* per chip volume. The reaction rate used in the current work is based on the kinetic model developed by Christensen *et al*. (1982).

2.3 Entrapped Liquor Phase Mass Continuity

It is assumed that the chips are saturated with water upon entering the digester. The water then mixes with reactants from free liquor that diffuse into the entrapped liquor and the dissolved reaction products from the solid phase. The entrapped liquor is, thus, an aqueous solution with six components: active effective alkali (EA) (e_1); passive EA (e_2); active hydrosulfide (HS) (e_3); passive HS (e_4); dissolved lignin (e_5) and dissolved carbohydrates (e_6). A component balance yields,

$$\frac{\partial \rho_{ei}}{\partial t} = -\frac{\rho_{ei}}{\varepsilon}\frac{\partial \varepsilon}{\partial t} + -\frac{v_c}{\varepsilon}\frac{\partial (\varepsilon \rho_{ei})}{\partial z} + D(\rho_{fi} - \rho_{ei}) + \hat{R}_{ei} \qquad (2)$$

Reaction rates, $\hat{R}_{ei}$ and $\hat{R}_{si}$, are related via stoichiometric constraints. ρ_{ei} represents concentration of entrapped liquor components defined as mass of component *i* in an elementary control volume per entrapped liquor volume. The third term on the right hand side of equation (2) models the diffusion of component *i* from the free liquor phase to entrapped liquor phase. Early Purdue developers (Smith and Williams, 1974; Christensen *et al.*, 1982) derived a correlation for the mass diffusion rate (defined on a volume basis), *D*, using experimental data for Kraft cooking presented in McKibbins (1960). Simulation results presented later are based on this correlation.

As suggested by Wisnewski *et al.* (1997), porosity of chips, $\varepsilon(z)$, is computed by comparing the density of solid phase components defined on chip volume basis with density of solid wood substance, $\overline{\rho}_s$, as follows,

$$\varepsilon(z) = 1 - \frac{\sum_{i=1}^{5} \rho_{si}(z)}{\overline{\rho}_s} \qquad (3)$$

In their work, Wisnewski *et al.* (1997) assume that the solids react and dissolve into the entrapped phase, contributing only mass and not volume. The newly created volume then sucks in free liquor from the neighboring free liquor phase. However, as discussed in section 2.7, this assumption violates volume continuity needed for calculation of compaction, η, and free liquor volumetric flowrates, $\dot{V}_f$. Thus, only the diffusive mechanism phase is retained as the means of mass transfer from the free liquor to the entrapped phase. Since, the entrapped liquor phase is incompressible, neglecting the vacuum effect amounts to assuming that the reacted solid components retain their density as in unreacted form in the solid phase.

The boundary conditions for the solid and entrapped phase continuity equations are fixed by the wood specie and the degree of impregnation.

2.4 Free Liquor Phase Mass Continuity

The free liquor phase is an aqueous solution of the same six components as in the entrapped liquor phase. Using the notation of Wisnewski *et al* (1997) for external flows, a component balance around the infinitesimal control volume gives the following,

$$\frac{\partial \rho_{fi}}{\partial t} = -v_c \frac{\partial \rho_{fi}}{\partial z} - D\varepsilon \frac{(1-\eta)}{\eta}(\rho_{fi} - \rho_{ei}) \pm \rho_{fi,ext} \frac{\dot{V}_{ext}}{\Delta V_f} \qquad (4)$$

The positive sign in the last term refers to external flows entering the control volume and negative for exiting flows. $\rho_{fi}(z)$ represents concentration of component *i* per volume of free liquor. The rate of diffusion of free liquor to entrapped phase is equal to that entering entrapped phase in equation (4) but expressed on a free liquor volume basis.

The boundary conditions for the free liquor continuity equations are provided by the concentrations of white liquor components in the cook zone and concentration of wash liquor components in the wash zone.

2.5 Chip and Free Liquor Thermal Energy Balances

Wisnewski *et al*. (1997) use mixing rules based on weighted averages to determine heat capacities of the

entrapped and free liquor phases. The same approach is retained in the current work. Below, energy balance equations modified to accommodate variable compaction are presented for the chip and free liquor phases and describe the temporal variation of the chip phase temperature T_c and free liquor temperature, T_f.

$$(C_{Ps}M_s + C_{Pe}M_e\varepsilon)\frac{\partial T_c}{\partial t} = -T_c\left(C_{Ps}\frac{\partial M_s}{\partial t} + C_{Pe}\frac{\partial (M_e\varepsilon)}{\partial t}\right) - v_c\frac{\partial}{\partial z}\left[(C_{Ps}M_s + C_{Pe}M_e\varepsilon)T_c\right] + \Delta H_R\sum_{i=1}^{5}\hat{R}_{si} + U(T_f - T_c) + D\varepsilon D_E \quad (5)$$

Heat released by the exothermic reactions between the entrapped liquor and solid phase components is modeled using the heat of reaction ΔH_R. Heat transfer coefficient U models the convective heat transfer between the chips and free liquor phases. Similarly, for the free liquor phase,

$$C_{Pf}M_f\frac{\partial T_f}{\partial t} = -T_f\frac{\partial}{\partial t}(C_{Pf}M_f) - v_f\frac{\partial}{\partial z}(C_{Pf}M_fT_f) - U\frac{(1-\eta)}{\eta}(T_f - T_c) - \frac{D\varepsilon(1-\eta)D_E}{\eta} \pm \frac{\dot{V}_{ext}M_{ext}T_{ext}}{\delta V_f} \quad (6)$$

The term $\frac{D\varepsilon(1-\eta)D_E}{\eta}$ represents the energy transfer to the chip phase per volume of diffusing mass.

Temperatures of wood chip charge, entering white liquor and entering wash liquor temperatures fix the boundary conditions needed for equations (5) and (6). Equations (1) to (6) are based on the work by Wisnewski *et al.* (1997) but modified to account for chip compaction and momentum balances. The reader is referred to that work as the primary source and also for a discussion of various modeling issues.

2.6 Chip Phase Volume Continuity

As discussed previously, progressive cooking of chips cause them to soften, thereby changing shape but not volume. The only mechanism that affects compaction of chips in a given control volume is the convective flow of chip phase. Thus, a volume balance for the elemental volume, ΔV, yields the following compaction equation,

$$\frac{\partial \eta}{\partial t} = \frac{\partial}{\partial z}\left[(1-\eta)v_c\right] \quad (7)$$

Michelsen's model includes axial dispersion in addition to convective flow of chips. However, subsequent steady-state analysis shows that the dispersion has a negligible effect on compaction. Michelsen also makes a degree of freedom argument to demonstrate how volume continuity follows from mass continuity. Boundary conditions for equation (7) is fixed by compaction of chips in a top section and is discussed in Section 2.10.

2.7 *Overall Digester Volume Continuity*

Equation (7) provides information on the fraction of the control volume occupied by chips. To satisfy overall digester volume continuity, the remainder of the volume must be occupied by free liquor. This in turn, prescribes the volumetric flowrate of free liquor as follows,

$$\nabla_z(\dot{V}_c + \dot{V}_f) = 0 \quad (8)$$

where the incoming and exiting external flows are included in the liquor flowrate. Equation (8) is an algebraic constraint expressing incompressibility of a control volume. It states that the sum of all flowrates entering a control volume of fixed size equals the sum of all flowrates exiting the volume. Bulk flow of free liquor into the entrapped phase by the vacuum effect discussed in section 2.3 decreases the flowrate of the exiting free liquor stream. However, no corresponding volume increase occurs in the chip phase thereby violating the incompressibility assumption.

We assume that the rate of extraction of the liquors from the cook and wash zone is perfectly controlled. These values are then used to compute the volumetric flow distribution using equation (8).

2.8 *Pressure Distribution in the Free Liquor Phase*

Calculation of the free liquor pressure distribution in presence of liquor velocity transients is a non-trivial task. Iterative methods (ex. SIMPLE algorithm, Patankar, 1980) exist in literature, which simultaneously arrive at a distribution of pressure and velocity fields such that the momentum and continuity equations are satisfied. However, the approach used here is to neglect free liquor momentum dynamics and utilize the resulting momentum equation to prescribe the pressure distribution. Michelsen (1995) suggests that this approach may be reasonable, since the period of free liquor velocity transients will be short due to incompressibility implied by equation (8).

Various forces affecting the system determine the free liquor pressure. Given the large capacity and height of the digester, gravity plays an important role in determining the liquor pressure. The remainder of the forces arise as a result of the viscous resistance faced by the chips as they flow through the liquor phase with a non-zero relative velocity. Härkönen, (1987) developed expressions for the resistive force based on the Ergun equation. He defined the resistive force as,

$$F_\Lambda = \Lambda\ v_{c,f} \tag{9}$$

where the coefficient of viscous friction is,

$$\Lambda = R_1 \frac{(1-\eta)^2}{\eta} + R_2 (1-\eta)\left|v_{c,f}\right| \tag{10}$$

and $v_{c,f}$ is the relative velocity between the chip and liquor phases. R_1 and R_2 are parameters estimated from experimental data. Neglecting inertial forces, the pressure distribution is calculated as,

$$\frac{\partial P_f}{\partial z} = -v_f \frac{\partial}{\partial z}\left[\rho_f v_f\right] - \eta v_f \frac{\partial \rho_f}{\partial t} + \rho_f g + \frac{F_\Lambda}{\eta} \tag{11}$$

The digester is assumed to be completely filled with liquor with a fixed pressure on the top. Equation (11) then provides the liquor pressure in the remainder of the digester column.

2.9 *Chip Phase Velocity Distribution*

In addition to the interphase flow resistance, Härkönen (1987) also modeled the chip pressure discussed in section 2.1 as a function of degree of cooking measured by Kappa # and compaction of chips, η as follows,

$$\begin{aligned} p_c &= 10^4 \left(\frac{(1-\eta) - 0.356}{0.831 - 0.139 \ln(\kappa)} \right)^{1.695} \quad \text{if } (1-\eta) < 0.356 \\ &= 0, \qquad \text{otherwise} \end{aligned} \tag{12}$$

For chip compaction below 35.6%, the chips float freely and do not exert pressure on adjacent chips. For a fixed compaction, the chip pressure decreases with increased cooking which corresponds to softening of the chips. The chip pressure also decreases with decreasing volume fraction of chips.

Michelsen (1995) models the force of sliding friction between the chip phase and the digester walls as,

$$F_\mu = \frac{4 \mu p_c}{D} \tag{13}$$

where μ is the coefficient of sliding friction and D_{cv} represents the diameter of the digester cross-sectional area. Using Newton's second law and combining the above forces, we get the axial chip velocity distribution as follows,

$$\begin{aligned} &\rho_c (1-\eta) \frac{\partial v_c}{\partial t} = -v_c (1-\eta) \rho_c \frac{\partial v_c}{\partial z} + \rho_c (1-\eta) g - \frac{\partial p_c}{\partial z} \\ &- (1-\eta) \frac{\partial p_c}{\partial z} - F_\Lambda - F_\mu \end{aligned} \tag{14}$$

Pulp production rate in the blowline fixes the boundary condition for the chip momentum equation.

2.10 *Chip Level*

Chip level constitutes one of the most important variables in digester control. It impacts the Kappa # via residence time of the chips in the digester. To model chip level, a top section of the digester is assumed, which covers a certain volume over the impregnation zone and consists of the chip phase interface. Chip phase inventory description then provides the dynamic description of level,

$$\dot{h}_c = \frac{1}{A(1-\eta_{top})} \left(\dot{V}_{c,feed} - A(1-\eta_0) v_{c,0} \right) \tag{15}$$

where η_{top} is an estimate of the compaction in the top section. Michelsen (1995) suggests using a linear relationship between the chip level and η_{top},

$$(1-\eta_{top}) = \begin{cases} 0.356 & \text{if } h_c < h_{\min} \\ 0.356 + k_{ts} h_c & \text{otherwise} \end{cases} \tag{16}$$

η_{top}, also forms the boundary condition for equation (7). Note that variables related to the bottom of the top section are indexed with zero, implying the beginning of the main section of the digester. Coefficient k_{ts} is determined empirically.

Equations (7) through (16) are primarily based on works by Härkönen (1987) and Michelsen (1995).

3. NUMERICAL METHOD

In this work the continuous domain model equations presented in section 2 are solved by replacing them with a finite difference mesh on a grid, such as shown in Fig. 3. Notation *j* refers to a fixed grid node on the digester vessel with the j^{th} control volume lying between nodes *j*-0.5 and *j*+0.5. Note that continuity balances are performed at half nodes while momentum balances for chip and liquor phase are performed at node *j* with *j*-0.5 and *j*+0.5 as the control volume boundaries (see Fig. 3). This overlapping of mass and momentum control volumes leads to a staggered grid approach and is routinely used in numerical fluid flow problems (Patankar,

1980). The approach ensures that only reasonable (non-wavy) pressure distributions are acceptable as solutions.

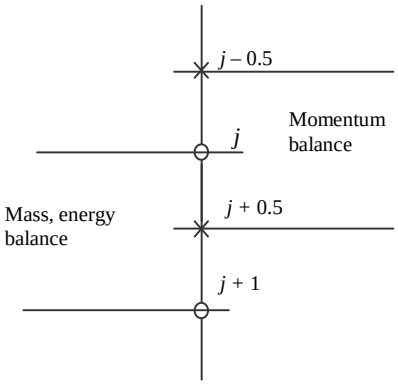

Fig. 3. Arrangement of overlapping control volumes on digester vessel

In the current model, axial transport of properties in the digester occurs by convection alone, resulting in a system of hyperbolic PDEs. It is well-known that solutions based on finite differences distort the information that is being convected downstream (Anderson *et al*, 1984). For example, simulation of a step-like change upstream of a flow system will exhibit dissipation or dispersion due to the truncation errors in the finite difference scheme, regardless of the modeling assumptions (see Fig. 4). To study the impact of the truncation errors, the spatial derivatives were differenced using two different schemes, viz. upstream differencing,

Fig. 4. Use of finite differences induce numerical diffusion

$$\frac{du_i}{dz} = \frac{u_i - u_{i-1}}{h} + O(z) \qquad (17)$$

and a fourth order difference formulation,

$$\frac{du_i}{dz} = \frac{-u_{i-3} + 6u_{i-2} - 18u_{i-1} + 10u_i + 3u_{i+1}}{12h} + O(z^4) \qquad (18)$$

where h represents the height of the finite control volume. Simulation results presented in the next section make use of the first order formula. An assessment of using the higher order formula is also presented.

4. SIMULATION RESULTS AND DISCUSSION

The simulations presented in this section are based on operating parameters presented in Table 5 in Wisnewski *et al*. (1997), except for the following differences: 1) the wash zone recirculation and bypass flowrates were set to zero; 2) the countercurrent cooling zone (see Fig. 1) is not modeled, and 3) the compaction profile is no longer constant. The digester was divided into 96 control volumes and equations (1) through (16) were implemented using Matlab/Simulink on a Sun Sparc Ultra 10, 333MHz workstation. A typical run simulating 80 hours of digester operation requires about 25 minutes of real time.

4.1 Steady State Behavior

The direct benefit of including momentum in the extended Purdue model is ability to simulate production rate changes. Fig. 5 shows comparisons between steady-state profiles of various digester variables for a low production rate (LPR) at 1.328 m^3/min and a high production rate (HPR) of pulp at 1.478 m^3/min (dashed line). The blowline flowrate step change was implemented using a first order filter with a time constant of 13 minutes. A simultaneous step change was introduced in the chip flowrate at top of the digester. This was necessary due to the integrating behavior of level dynamics. The reduced residence time of chips leads to lower extent of conversion of lignin (Fig. 5a) and a corresponding increase in Kappa # (Fig. 5f). The Kappa # shows an initial increase in the impregnation zone (z<0.14) and a subsequent decrease in the cooking zone (0.14<z<0.75). Figs. 5b-5d show components of entrapped and free liquor. The increase in blowline flow reduces available time for diffusion of EA and HS from free liquor to the entrapped phase leading to a drop in concentrations in the entrapped phase. However, this increases the concentration driving force, which in turn causes the free liquor concentrations to drop as well. Volume fraction of liquor (Fig. 5g) increases in the vicinity of the extraction screen, implying loose packing of chips. This is a result of lower degree of cooking or higher Kappa # and is consistent with Michelsen's argument of Kappa # and compaction. The lower compaction of chips results in lowering of liquor velocities (Fig. 5i), as more area is available for the free liquor flow. The increase in chip velocity (Fig. 5h) is a result of

higher volumetric throughput. Figs. 5j,k,l show the temperatures of chip and liquor, and chip porosity, respectively.

Steady-state compaction and Kappa # profiles for a filtered step increase in white liquor flowrate are shown in Fig. 6. The figure highlights the situation where excessive cooking may nearly cause the digester to plug up near the extraction screen. This is the result of dense packing of cooked chips. The counter flow of dilute liquor aids in dispersing the fibers as the pulp enters the wash zone.

4.2 Dynamic Behavior

Fig 7 shows results for filtered step changes in (1) blowline flow, (2) cooking circulation upper heater, (3) white liquor and (4) dilute liquor flows of 0.15 m^3/min, -10 ^oC, -0.15 m^3/min and -0.15 m^3/min, respectively. In each of the cases, the relation between the endpoint Kappa # and chip level is apparent, as they are coupled via residence time. The decrease in the chip level in case 4 is due to the lower "lift" provided by the reduced dilute liquor flowrate. Cases 2) and 3) show kinks and overshoots in the endpoint Kappa # plot while traversing from the initial steady state to the final steady state. No simple mechanistic explanation emerges from the dynamic equations. Upon an analysis of simulations, it is observed that the oscillations first appear in the Kappa # and chip velocity when the upper heater temperature is perturbed (Fig. 8). The initial increase in Kappa # is accompanied by a retardation of chip velocity due to increased chip pressure, which propagates downstream giving rise to the oscillatory behavior in the Kappa #. However, further investigation needs to be performed to assess if the oscillations have a phenomenological explanation or are merely artifacts of the numerical method. Specifically, it must be determined if numerical diffusion caused by the finite difference approach to approximate convective transport plays any role in producing the oscillatory response. Fig. 9 shows comparisons for steps in white liquor and dilute liquor flows in opposite directions. Although the process gains are seen to be nonlinear, the dynamic response exhibit symmetry.

4.3 Assessment of Higher Order Numerical Method

To study the impact of using a higher order numerical method on variables of interest such as endpoint Kappa #, the following experiment was performed. The simulation based on the first order difference method (equation (17)) was allowed to reach steady state after which the fourth order scheme (equation (18)) was used without changing any operating conditions or model parameters. Fig. 10 depicts the results. It is noted that the higher order formulation predicts increased conversion of lignin leading to a drop in Kappa # by about 3. Use of the first order method approximates the digester as a series of CSTRs. However, chip flow in the digester more closely resembles plug flow since backmixing is absent. It is known that the CSTR usually accomplishes lower conversion for a given volume than the plug flow reactor (Fogler, 1999). Thus, the increased conversion with the higher order method is consistent with the fact that the fourth order finite difference formula provides a better approximation of the plug flow behavior in the digester.

5. CONCLUSIONS

In this work, a thermal-hydraulic model of the digester has been presented. The model provides a detailed description of the important phenomena involved in operating the digester using conservation laws. Constitutive rules were adopted from available literature (Christensen *et al.* 1982; Härkönen, 1987). Pulping chemistry was based on the Purdue model while the hydraulics mainly rely on work by Härkönen (1987). Thus, the work constitutes a hydraulic extension of the Purdue model.

Simulation examples demonstrated various attributes of the model. While no rigorous validation exercise was performed, the variable trends follow those of extended Purdue model (Wisnewski, 1997) where applicable and can be explained mechanistically. The benefits of the hydraulic extension are, however, realized in the ability of the model to explain the impact of dynamic flowrate and compaction changes on the pulp quality. Moreover, the chip level, an important control variable is one of the model outputs.

Use of a higher order finite difference formula for the spatial derivative reveals increased conversion. This observation is consistent with the fact that the higher order scheme is a better approximation of the plug flow behavior.

6. ACKNOWLEDGEMENT

The authors acknowledge funding from the Department of Energy (Grant DE-FC07-00ID-13882).

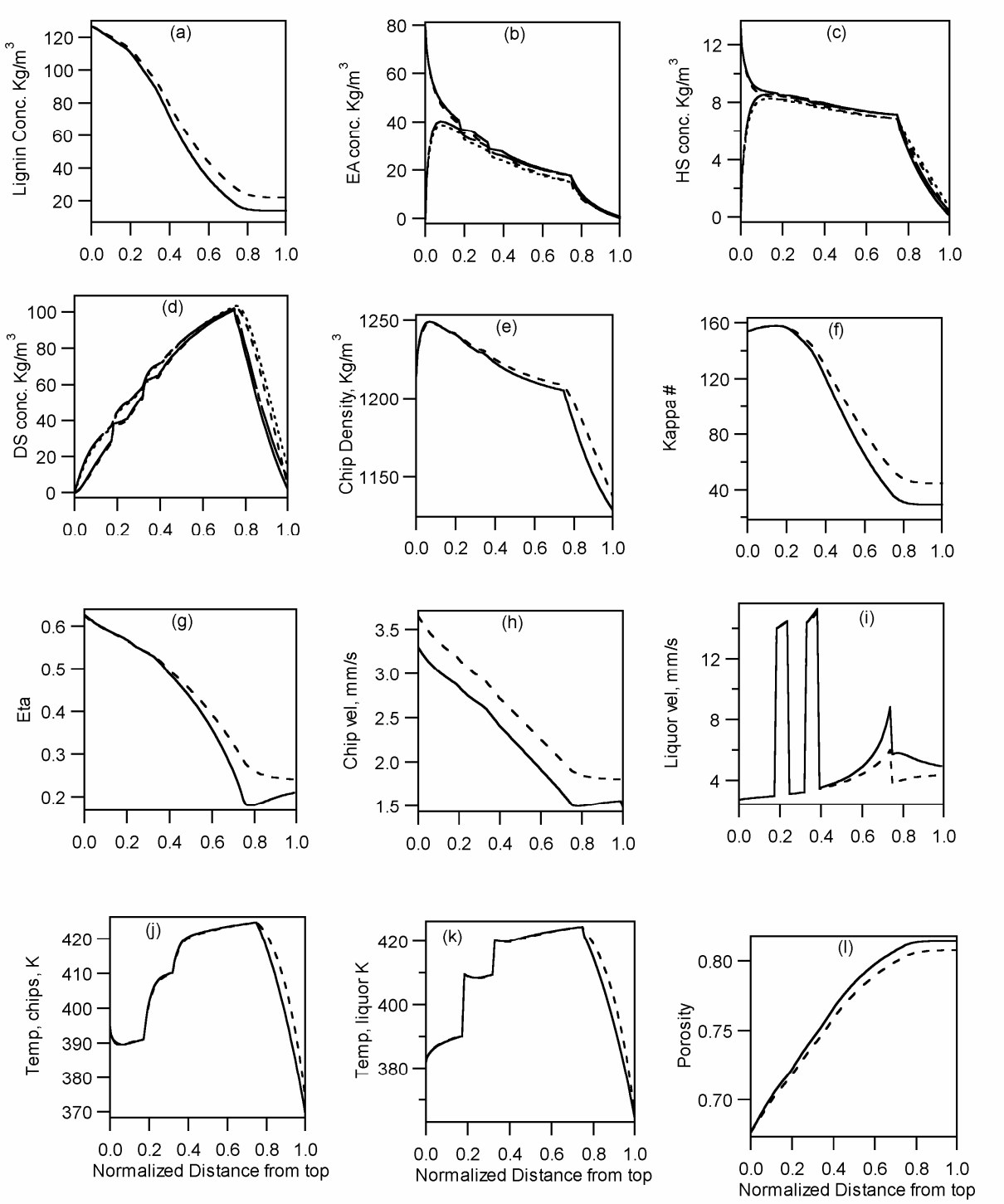

Fig 5. Steady state behavior for low (solid) and high (dashed) blowline flowrates. Impregnation zone: $z<0.14$; : cook zone: $0.14 \le z < 0.75$: wash zone: $z \ge 0.75$.

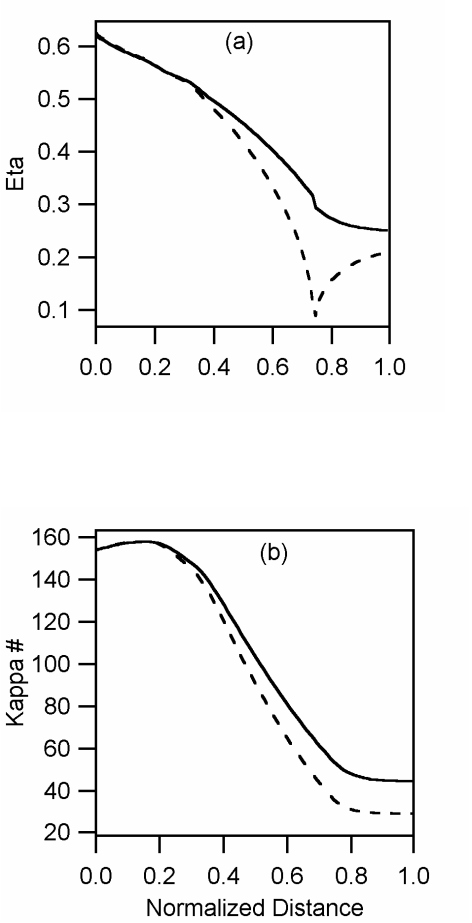

Fig. 6. Steady state compaction and Kappa # profiles for low (solid) and high (dashed) values of white liquor flowrates.

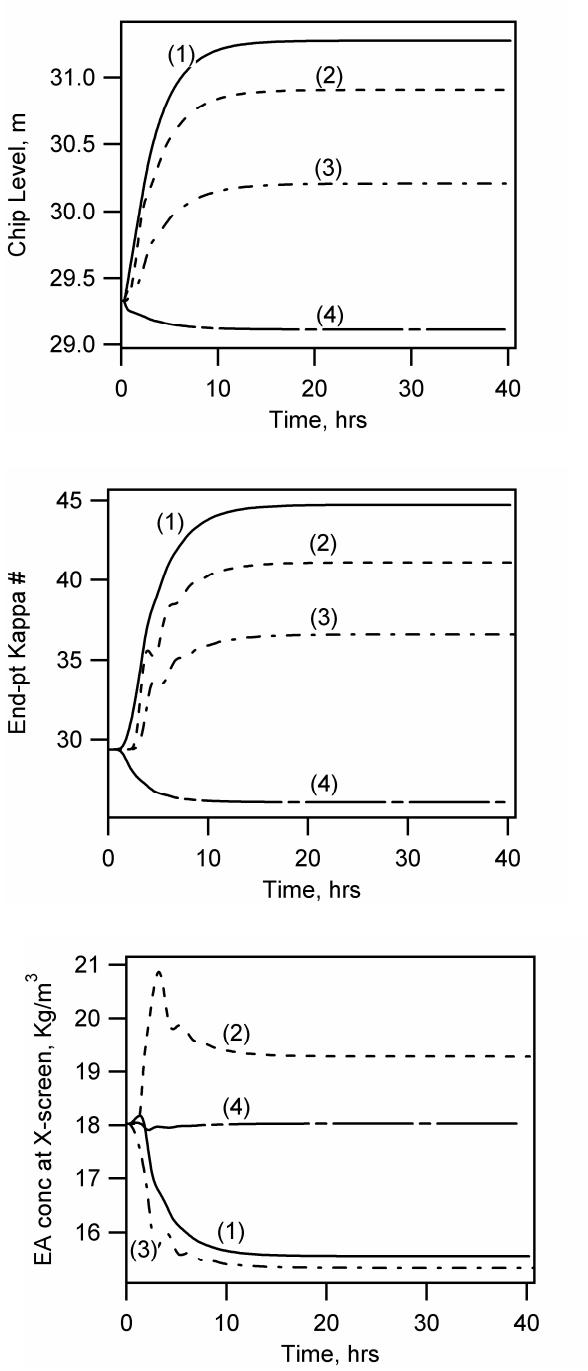

Fig. 7. Dynamic behavior for (1) increase in blowline flow; (2) decrease in upper heater temp.; (3) decrease in white liquor; and (4) decrease in dilute liquor flow.

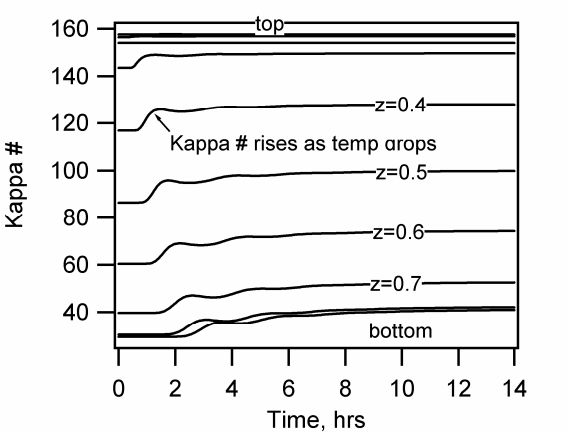

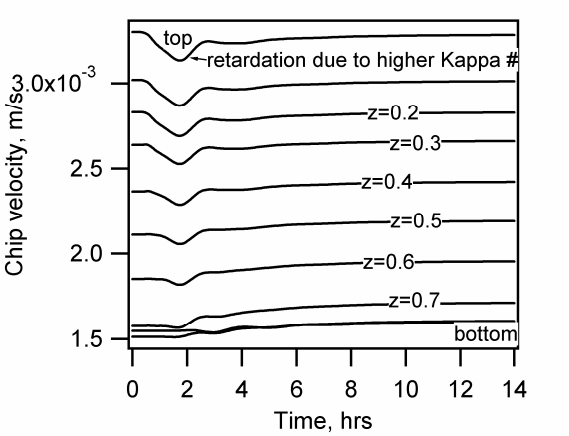

Fig. 8. Velocity and Kappa # transients at various locations on the digester due to change in upper heater circulation temperature ("top" and "bottom" refer to the digester).

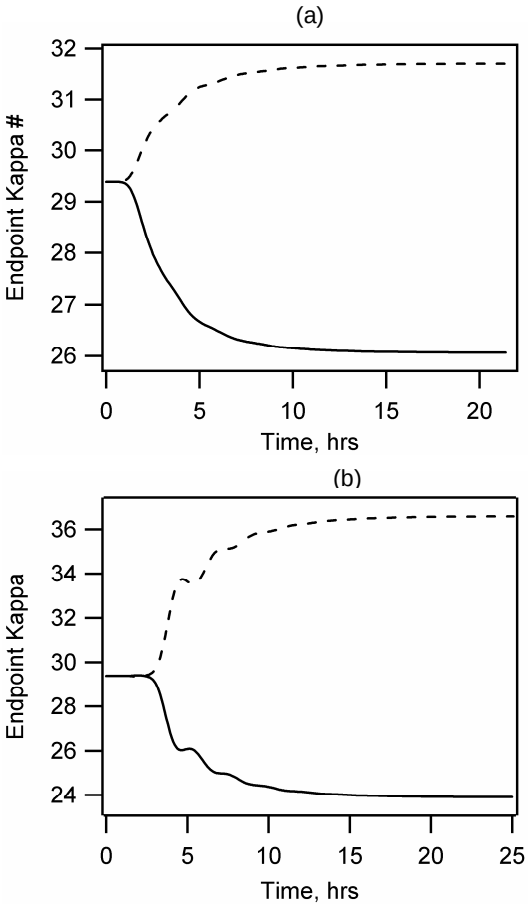

Fig. 9. Symmetric step tests for (a) ±0.15 m^3/min change in dilute liquor flow; and (b) ±0.15 m^3/min change in white liquor flow

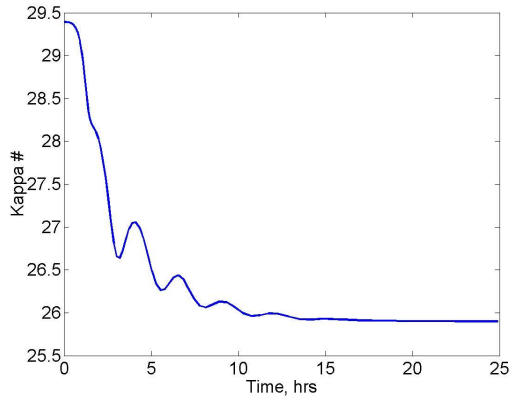

Fig. 10. Higher order numerical method predicts higher removal of lignin from chips.

REFERENCES

Anderson, D.A., J.C. Tannehill and R.H.Pletcher (1984). Computational Fluid Mechanics and Heat Transfer, *McGraw Hill*, New York.

Christensen, T., L.F. Albright and T.J. Williams (1982). A Mathematical Model of the Kraft Pulping Process, *Tech. Rep. 129* Purdue University,PLAIC, West Lafayette, Indiana.

Christensen, T., M. Ivan, R. Michelsen, G. Lunde and U. Zetterlund (1994). Model Predictive Control of a Continuous Kamyr Digester, *Pulp and Paper Canada*, **95**, 146.

Fogler, H.S.(1999). Elements of Chemical Reaction Engineering, 3rd ed, *Prentice Hall*, New Jersey.

Gustafson, R., C. Sleicher, W. McKean and B. Finlayson (1983). Theoretical Model of the

Kraft Pulping Process, *Ind. Eng. Chem. Proc. Des. Dev.*, **22**, 87.

Härkönen, E.J., (1987). A Mathematical Model for Two-Phase Flow in a Continuous Digester, *TAPPI J.*, **70**, 122.

Kayihan, F., M.S. Gelormino, E.M. Hanczyc, F.J. Doyle III, and Y. Arkun (1996). A Kamyr continuous digester model for identification and controller design, *Proc. IFAC World Congress*, San Francisco, 37.

McKibbins, S.W., (1960). Application of Diffusion Theory to the Washing of Kraft Cooked chips, *Tappi J.*, **43**, 801.

Michelsen, F.A., (1995) A Dynamic Mechanistic Model and Model-Based Analysis of a Continuous Kamyr Digester, *Ph.D. Thesis*, University of Trond heim.

Patankar, S., (1980). Numerical Heat Transfer and Fluid Flow, McGraw Hill, New York.

Smith, C.C., and T.J. Williams, (1974). Mathematical Modeling, Simulation and Control of the Operation of Kamyr Continuous Digester for Kraft Process, *Tech. Rep 64*, Purdue University, PLAIC, West Lafayette, Indiana.

Wisnewski, P.A., F.J. Doyle III, and F. Kayihan, (1997), Fundamental Continuous Pulp Digester Model for Simulation and Control, *AIChE J.*, **43**, 3175.